arXiv:2110.00205v4 [gr-qc] 10 Mar 2023

NANOGrav Signal from double-inflection-point inflation and dark matter

Tie-Jun Gao*

School of Physics and Optoelectronic Engineering,

Xidian University, Xi'an 710071, China

Abstract

The NANOGrav collaboration has published a suspected stochastic GW background signal in its analysis of 12.5 years PTA data, so in this work, we investigate the possibility to explain the signal by the inflationary models with double-inflection-point. We calculate the energy spectrum of GWs induced by scalar perturbations, and show that the curve lies in the 2σ region of the NANOGrav constraints. In addition, we analyze the reheating process and dark matter production by assuming that the inflaton is coupled with the SM Higgs boson and singlet fermionic dark matter field. We discuss the radiative stability of the inflationary potential under one-loop corrections, calculate the reheating temperature, the dark matter production, and constraints the coupling parameters using the bounds of BBN, Lyman-α, etc.

Keywords: inflation, gravitational waves, dark matter

* tjgao@xidian.edu.cn

I. INTRODUCTION

Recently, the North American Nanohertz Observatory for Gravitational Waves (NANOGrav) has published its 12.5 years observation data of pulsar timing array(PTA), where strong evidence of a stochastic process, which can be explained by the stochastic gravitational waves (GWs) with a power-law spectrum $\Omega_{GW} \propto f^{5-\gamma}$ at a reference frequency of $f_{yr} \simeq 3.1 \times 10^{-8}$Hz, with the exponent $5-\gamma \in (-1.5, 0.5)$ at 1σ confidence level[1–7].

It has been pointed out in several literatures that if the power spectrum of scalar perturbations has a large peak at low scales, then when the perturbations corresponding to the peak renters the horizon during the radiation-dominated period, it will induce GWs, which is sizable to be detectable by experiments in near future[8–22]. Such enhancement of the power spectrum can be achieved in the ultra-slow-roll phase near the inflection point in some inflationary models [23–28], and similar models have been discussed in many literatures [29–31],or in the framework of string theory [32–35] etc. However, In the previous models, the potential contains single inflection point, and the inflation will last about more than 30 e-folding numbers before the inflection point. Thus near the inflection point, the peak of the power spectrum will induced GWs around millihertz, which couldn't explain the NANOGrav result around nanohertz. So in this paper, motivated from the framework of effective field theory, we consider a polynomial potential model with double-inflection-point. In such a model, the inflection point at CMB scales can make the predictions consistent with the 2018 data[36] and last about 20 e-folding numbers, thus when the inflaton meets the second inflection point, it will induce GWs with the peak around nanohertz, which can explain the NANOGrav signal.

After inflation ends, the inflaton will oscillate around the minimum of the potential and decay into relativistic particles, which will reheating the universe. So in this paper, we assume that the inflaton can decay into the standard model(SM) Higgs boson or decay into singlet fermions beyond SM, which can be a component of dark matter(DM). In order to ensure that the effect of the added coupling terms do not affect the inflationary dynamics at the CMB scale,and do not affect the GW energy spectrum, we discuss the radiative corrections at one-loop order using the Coleman-Weinberg (CW) formalism [37, 38]. We also

calculate the reheating temperature and constraint the model parameters using BBN[39–43], Lyman-α [44, 45], etc. We also analysis the dark matter production, and show that the main way to produce dark matter is the direct decay of inflatons.

The paper is organized as follows. In the next section, we setup the inflationary model with double-inflection-point using a scalar potential with polynomial form. In Sec.3, we analyze the inflation dynamics of the model and calculate the power spectrum numerically. In Sec.4, we calculate the energy spectrum of the induced GWs and compared the results with NANOGrav and some planned experiments. In Sec.4, we assume that after inflation, the inflaton will decay into SM Higgs or singlet fermionic field and analyze the reheating temperature. We also calculate the effect of one-loop corrections of the coupling terms in Sec.5. In Sec. 6, we discuss the dark matter production and calculate the relic density. The last section is devoted to summary.

II. THE DOUBLE-INFLECTION-POINT MODEL

In this section, we consider a scalar potential with polynomial form, which can generate an inflationary model with double-inflection-point. Such a polynomial can be derived from the effective field theory with a cutoff scale Λ [46–51]

$$V_{\text{eff}}(\phi) = \sum_{n=0} \frac{b_n}{n!} \left(\frac{\phi}{\Lambda}\right)^n . \tag{1}$$

To obtain a inflationary potential containing double-inflection-point, we truncate the above polynomial to the sixth order, and redefine the parameters as

$$V(\phi) = V_0 \left[c_2 \left(\frac{\phi}{\Lambda}\right)^2 + c_3 \left(\frac{\phi}{\Lambda}\right)^3 + c_4 \left(\frac{\phi}{\Lambda}\right)^4 + c_5 \left(\frac{\phi}{\Lambda}\right)^5 + \left(\frac{\phi}{\Lambda}\right)^6 \right], \tag{2}$$

where the overall factor V_0 can be constrained by the amplitude of scalar perturbations A_s, and we have omit the constant and first-order terms of the polynomial so that the potential and it's first-order derivative vanish at the origin. By tuning the four dimensionless parameters c_{2-5} one can obtain a potential with two inflection points.

For the purpose of discussion, we assume that the two inflection points are located at $\phi_i (i = 1, 2)$, where the first and second derivatives of V vanish,i.e. $V'(\phi_i) = 0$ and $V''(\phi_i) =$

0. This condition yields the following relationship between c_{2-5} and ϕ_i

$$c_2 = \frac{3}{\Lambda^4}\phi_1^2\phi_2^2, c_3 = \frac{-4}{\Lambda^3}\left(\phi_1^2\phi_2 + \phi_1\phi_2^2\right), c_4 = \frac{3}{2\Lambda^2}\left(\phi_1^2 + 4\phi_1\phi_2 + \phi_2^2\right), c_5 = \frac{-12}{5\Lambda}(\phi_1 + \phi_2). \quad (3)$$

However, in order to obtain a reasonable model, the inflection points of the potential are not strict, so we introduce two additional parameters α_i to represent the small deviation. Then the scalar potential can be written in the following form

$$\begin{aligned} V(\phi) =& \frac{V_0}{\Lambda^6}\Big(3\phi_1^2\phi_2^2\phi^2 - 4\left(\phi_1^2\phi_2 + \phi_1\phi_2^2\right)(1+\alpha_1)\phi^3 \\ &+ \frac{3}{2}\left(\phi_1^2 + 4\phi_1\phi_2 + \phi_2^2\right)\phi^4 - \frac{12}{5}(\phi_1+\phi_2)(1+\alpha_2)\phi^5 + \phi^6\Big). \end{aligned} \quad (4)$$

For some parameter spaces, the model is both consistent with the CMB observational constraints and interprets the NANOGrav signal. For instance, we choose

$$\begin{aligned} &V_0 = 2.157 \times 10^{-13} M_p^4, \quad \Lambda = M_p, \\ &\phi_1 = 0.9095875 M_p, \qquad \alpha_1 = 8.5654 \times 10^{-5}, \\ &\phi_2 = 2.10081 M_p, \qquad \alpha_2 = -4.0172 \times 10^{-5}, \end{aligned} \quad (5)$$

which corresponds to the parameters c_{2-5} are

$$c_2 = 10.9543,\ c_3 = -23.0119,\ c_4 = 19.3264,\ c_5 = -7.22466. \quad (6)$$

In Fig. 1 we draw the corresponding potential, which contains double-inflection-point. As we will see below, the inflation starts near the first inflection point at high scale and generates a nearly scale-invariant power spectrum, which is in good agreement with the CMB observations, and when the inflaton rolls near the second inflection point at low scale, it will go through an ultra-slow-roll phase, which will last about 35 e-folding numbers and resulting in a large peak in the power spectrum, which will induces gravitational waves consistent with the NANOGrav data.

III. INFLATION DYNAMICS

In this section, we will discuss the dynamics of inflation. Since there is an ultra-slow-roll stage in the process of inflation, so in order to calculate the power spectrum more accurately,

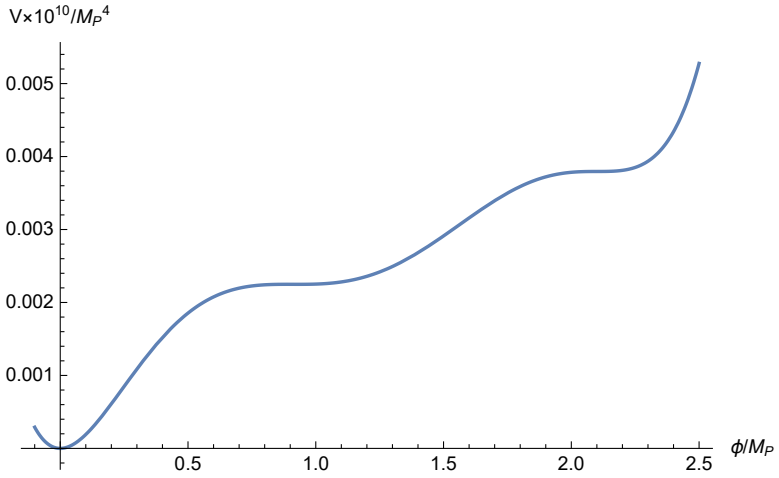


FIG. 1: The scalar potential with parameter set (5).

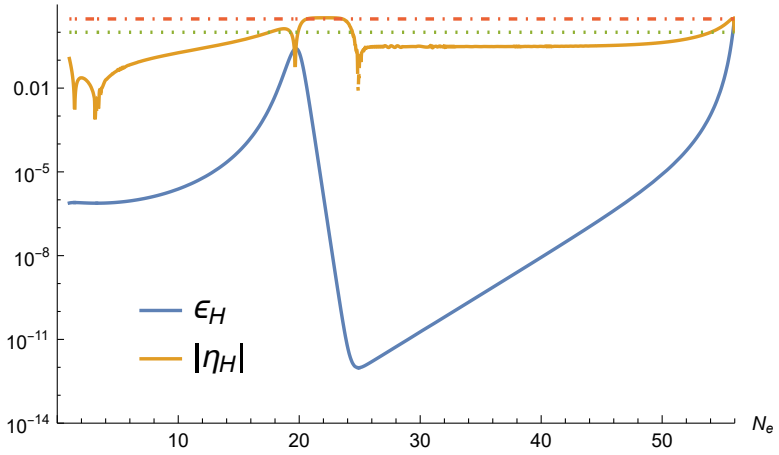


FIG. 2: The Hubble slow-roll parameters ϵ_H and η_H as functions of the e-folding number N_e. The green and red dashed lines represent 1 and 3, respectively.

we use the Hubble slow roll parameters defined below [52–58]

$$\epsilon_H = -\frac{\dot{H}}{H^2},$$
$$\eta_H = -\frac{\ddot{H}}{2H\dot{H}} = \epsilon_H - \frac{1}{2}\frac{d\ln\epsilon_H}{dN_e}, \tag{7}$$

with dots represent derivatives with respect to the cosmic time, and N_e is the e-folding numbers. The corresponding curves of ϵ_H and η_H with respect to N_e are shown in Fig.2, and the evolution of Hubble parameter with respect to N_e are shown in Fig.3.

As we can see in the figure, near the second inflection point, the slow-roll parameter

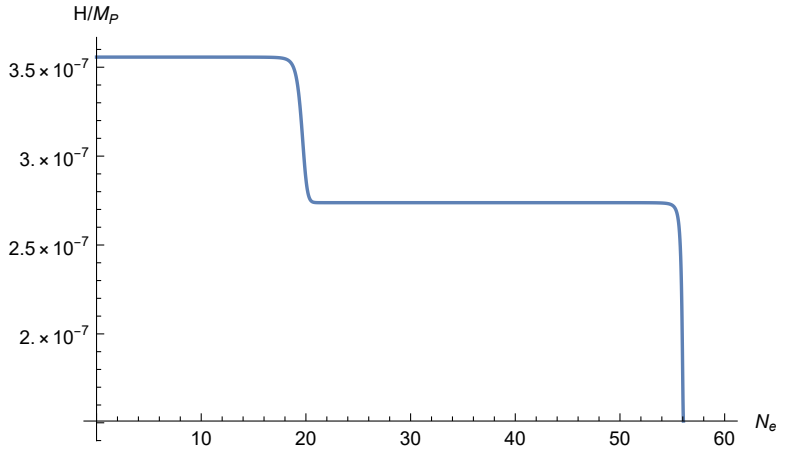


FIG. 3: The Hubble parameters as functions of the e-folding number N_e

$|\eta_H| > 3$, which implies that inflation undergoes an ultra-slow-roll process. Correspondingly, the curve of the slow-roll parameter ϵ_H appears a deep valley lasting about 30 e-folding numbers, which will make the power spectrum appear a large peak. In order to calculate the power spectrum at the ultra-slow-roll process, the slow-roll approximation is no longer applicable, so the Mukhanov-Sasaki(MS) equation of mode function u_k, must be solved strictly [26]

$$\frac{d^2u_k}{d\tau^2} + \left(k^2 - \frac{1}{z}\frac{d^2z}{d\tau^2}\right)u_k = 0, \tag{8}$$

with $z \equiv \frac{a}{\mathcal{H}}\frac{d\phi}{d\tau}$, and τ denotes the conformal time. And the initial condition is taken to be the Bunch-Davies type[59]

$$u_k \to \frac{e^{-ik\tau}}{\sqrt{2k}}, \quad \text{as} \quad \frac{k}{aH} \to \infty. \tag{9}$$

Then the power spectrum are calculated by

$$\mathcal{P}_\mathcal{R} = \frac{k^3}{2\pi^2}\left|\frac{u_k}{z}\right|^2_{k\ll aH}. \tag{10}$$

We show the numerical result(blue line) and the approximate results(orange line) of the scalar power spectrum in Fig.4. And the constraints to the primordial power spectrum from μ-distortion of CMB are also show there. We can see that the ultra-slow-roll behavior near the inflection point leads to a large peak in the power spectrum, and the peak value is about seven orders of magnitude higher than the power spectrum of the CMB scale. We will see in

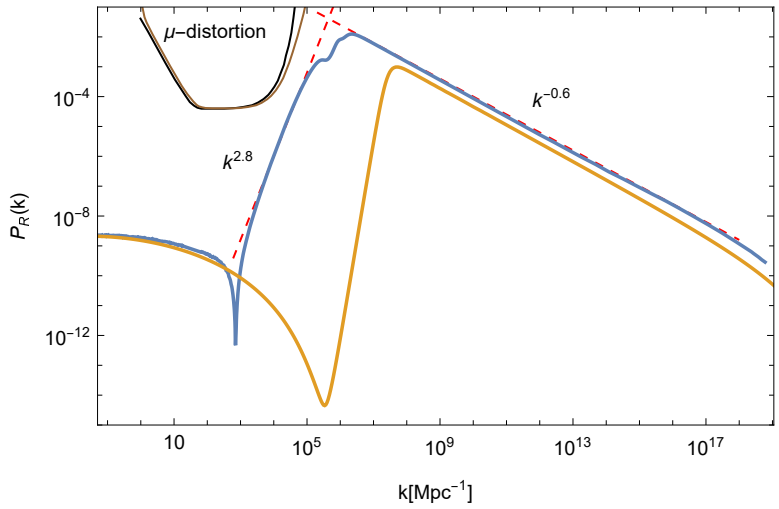


FIG. 4: The power spectrum of scalar perturbations with the parameter set(5). And the black and brown lines show the upper bound from μ-distortion for a delta function power spectrum and for the steepest growth k^4 power spectrum, respectively[60].

the next section that the perturbations corresponding to the peak will induce experimentally detected GWs after re-entering the horizon, and can explain the signal of NANOGrav.

In order to verify that the model agrees with the constraints of Planck experiment on CMB scale, we estimate the corresponding scalar spectral index and the tensor-to-scalar ratio, which can be expressed using ϵ_H and η_H at the leading order as

$$\begin{aligned} n_s &= 1 - 4\epsilon_H + 2\eta_H, \\ r &= 16\epsilon_H. \end{aligned} \tag{11}$$

The numerical results are $n_s = 0.9672$, $r = 1.22 \times 10^{-5}$, and the amplitude of the primordial curvature perturbations A_s and the e-folding numbers during inflation N_e are $\ln(10^{10} A_s) = 3.0444$, $N_e = 56.6$. The results are all consistent with the observation constraints from Planck 2018, which are $n_s = 0.9649 \pm 0.0042$, $r < 0.064$ and $\ln(10^{10} A_s) = 3.044 \pm 0.014$[36].

IV. INDUCED GRAVITATIONAL WAVES

In the following, we will numerical calculate the second order GWs induced by scalar perturbations using the power spectrum obtained in the province subsection. When the

scalar perturbation re-enters the horizon, it will induce second-order GWs[61–66], and the corresponding GW energy spectrum can be expressed by the tensor power spectrum as

$$\Omega_{\rm GW}(\tau,k)=\frac{1}{24}\left(\frac{k}{\mathcal{H}}\right)^2\overline{\mathcal{P}_h(\tau,k)}\,, \tag{12}$$

where the overline denotes the oscillation average among several wavelengths. Using the Green's function method and considering that $\mathcal{H}=1/\tau$ in the radiation dominant period, the above energy spectrum can be calculated by the scalar power spectrum as following [13]

$$\begin{aligned}\Omega_{\rm GW}(\tau,k)=&\frac{1}{12}\int_0^\infty dv\int_{|1-v|}^{1+v}du\left(\frac{4v^2-(1+v^2-u^2)^2}{4uv}\right)^2\mathcal{P}_{\mathcal{R}}(ku)\mathcal{P}_{\mathcal{R}}(kv)\\&\left(\frac{3}{4u^3v^3}\right)^2\left(u^2+v^2-3\right)^2\\&\left\{\left[-4uv+\left(u^2+v^2-3\right)\ln\left|\frac{3-(u+v)^2}{3-(u-v)^2}\right|\right]^2+\left[\pi\left(u^2+v^2-3\right)\Theta(u+v-\sqrt{3})\right]^2\right\},\end{aligned} \tag{13}$$

where u and v are two dimensionless variables. Finally, the energy density spectrum of GWs today $\Omega_{\rm GW,0}$ is calculated by[63]

$$\Omega_{\rm GW,0}=0.83\left(\frac{g_*}{g_{*,p}}\right)^{-1/3}\Omega_{r,0}\Omega_{\rm GW}, \tag{14}$$

with $\Omega_{r,0}\simeq 9.1\times10^{-5}$ is the energy density fraction of radiation at present, g_* and $g_{*,p}$ denote the effective number of degrees of freedom for energy density today and at the horizon crossing, respectively.

Combine the numerical result of scalar power spectrum $\mathcal{P}_{\mathcal{R}}$ obtained in the previous subsection, we numerically calculate the energy spectrum of induced GWs and show it in Fig.5, with the horizontal axis is the frequency at present

$$f\approx 0.03{\rm Hz}\frac{k}{2\times10^7{\rm pc}^{-1}}. \tag{15}$$

And the upper curves are the sensitivity curves of some planned GW detectors [31, 67–71].

Recently, the NANOGrav collaboration has published its 12.5-year data of PTA, which indicate a signal which can be explained by the stochastic GWs with a power-law spectrum around $f_{yr}\simeq 3.1\times10^{-8}$Hz,

$$\Omega_{GW}(f)=\frac{2\pi^2f_{yr}^2}{3H_0^2}A_{GWB}^2\Big(\frac{f}{f_{yr}}\Big)^{5-\gamma}, \tag{16}$$

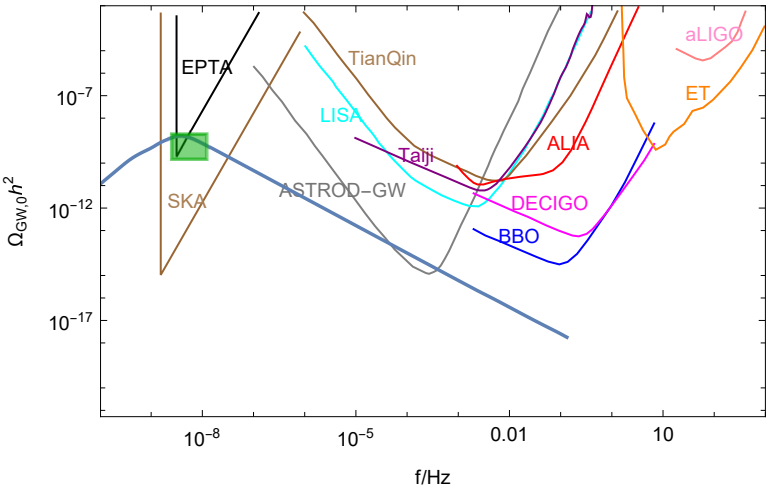


FIG. 5: Energy spectrum of the induced GWs at the present time predicted by the polynomial model for parameter set (5). The curves in the upper part are the expected sensitivity curves of the European Pulsar Timing Array (EPTA), Square Kilometer Array (SKA),Laser Interferometer Space Antenna (LISA),Taiji, TianQin,Astrodynamical Space Test of Relativity using Optical-GW detector (ASTROD-GW), Advanced Laser Interferometer Antenna (ALIA), Big Bang Observer (BBO), Deci-hertz Interferometer GW Observatory (DECIGO),Einstein Telescope (ET), Advanced LIGO (aLIGO), respectively. These sensitivity curves are taken from Ref. [31, 67–71] The green region show the 2σ confidence level of the NANOGrav results with the tilt of $5-\gamma=0$[1].

where $H_0 \equiv 100h$ km/s/Mpc, and $5-\gamma \in (-1.5, 0.5)$ at 1σ confidence level[1–7]. The observed GWs for $5-\gamma=0$ with 2σ uncertainty on A_{GWB} are also show in Fig.5.

We can see that the frequencies of the spectrum of GWs cover from nanohertz to millihertz, and the maximum is at the frequency $f = 3.97 \times 10^{-9} Hz$, which is within the frequency range of SKA and EPTA. The the spectrum of induced GWs with frequencies around nanohertz lies in the 2σ region of the NANOGrav constraints, so it can explain the NANOGrav signals. And around millihertz, the energy spectrum curves lies above the expected sensitivity curves of ASTROD-GW, so it can be tested by the observation in near future.

V. REHEATING

After inflation ends, the inflaton rolls down the potential and then oscillates around the minimum, and the energy of inflaton will transfers to other degree of freedoms and raises the temperature of the universe. This is known as the reheating period. Following Reference [72–74], we consider the inflaton decays into SM Higgs boson or decays into a Dirac fermion χ through trilinear coupling, which can be a candidate of DM. The additional terms in the Lagrangian density has the following form

$$\mathcal{L} = i\bar{\chi}\gamma^{\mu}\partial_{\mu}\chi - m_{\chi}\bar{\chi}\chi - y_{\chi}\phi\bar{\chi}\chi - \lambda_{12}\phi H^{\dagger}H - \frac{1}{2}\lambda_{22}\phi^{2}H^{\dagger}H, \tag{17}$$

where m_{χ} is the mass of the DM, the coupling coefficient y_{χ}, λ_{22} are dimensionless and λ_{12} has a dimension of mass. The associated decay widths are

$$\begin{aligned} \Gamma_{\phi\to H^{\dagger}H} &\simeq \frac{\lambda_{12}^{2}}{8\pi m_{\phi}}, \\ \Gamma_{\phi\to\bar{\chi}\chi} &\simeq \frac{y_{\chi}^{2}m_{\phi}}{8\pi}, \end{aligned} \tag{18}$$

with $m_{\phi}^{2} = \frac{\partial^{2}V}{\partial\phi^{2}}|_{\phi=0}$ is the inflaton mass during reheating, and we have assumed that the mass of χ and H are much smaller then m_{ϕ}. In order to fit the relic density of photon numbers and hadronic numbers today, the decay width to the SM Higgs boson should be much greater than the decay width to the fermionic DM, that is the total decay width of the inflaton be approximated as $\Gamma \equiv \Gamma_{\phi\to H^{\dagger}H} + \Gamma_{\phi\to\bar{\chi}\chi} \simeq \Gamma_{\phi\to H^{\dagger}H}$. Therefore branching ratio of DM production can be calculated as follows

$$\mathrm{Br} \equiv \frac{\Gamma_{\phi\to\bar{\chi}\chi}}{\Gamma_{\phi\to H^{\dagger}H} + \Gamma_{\phi\to\bar{\chi}\chi}} \simeq \frac{\Gamma_{\phi\to\bar{\chi}\chi}}{\Gamma_{\phi\to H^{\dagger}H}} \simeq m_{\phi}^{2}(\frac{y_{\chi}^{2}}{\lambda_{12}^{2}}). \tag{19}$$

During reheating, when the Hubble parameter becomes small enough, the energy loss due to the decay of the inflaton is greater than the energy loss due to the expansion of the universe, the corresponding temperature when $H = \frac{2}{3}\Gamma$ is defined as the reheating temperature T_{rh}. In the instantaneous decay approximation the reheating temperature can be calculated as [73]

$$T_{rh} = \sqrt{\frac{2}{\pi}}\left(\frac{10}{g_{*}}\right)^{1/4}\sqrt{M_{P}}\sqrt{\Gamma}, \tag{20}$$

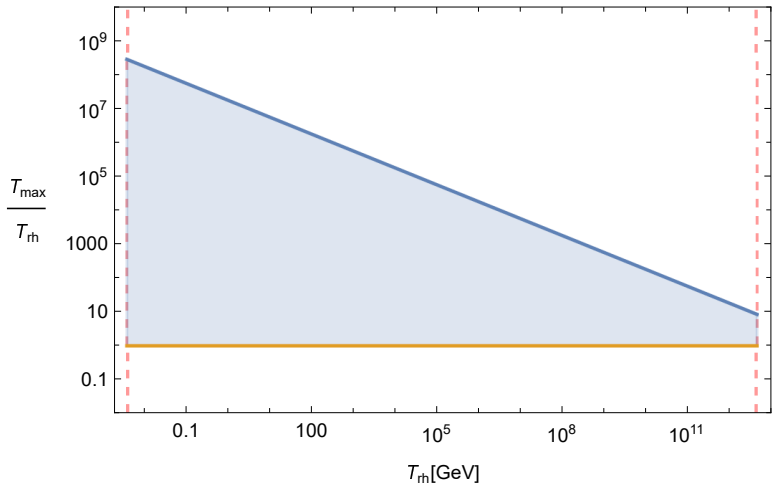


FIG. 6: The allowed ranges of the ratio $T_{\max}/T_{rh}$.

where Γ is the total decay width of the inflaton, and $g_* = 106.75$. And the maximum temperature during reheating can be calculated by [75–77]

$$T_{\max} = \Gamma^{1/4} \left(\frac{60}{g_* \pi^2}\right)^{1/4} \left(\frac{3}{8}\right)^{2/5} H_I^{1/4} M_P^{1/2}, \tag{21}$$

where H_I is the Hubble parameter at the beginning of reheating. In our model, according to Fig.3, we use the value around the second inflection point.

According to the restriction of BBN, the reheating temperature T_{rh} should be greater than 4MeV[39–43]. Moreover, the Planck 2018 give an upper limit on the inflation scale $H_I \leq 2.5 \times 10^{-5} M_p$ [36], which would allows an upper limit on the reheating temperature $T_{rh} \leq 7 \times 10^{15}$GeV. So we can give the limit of the coupling parameter λ_{12} according to equation (20)

$$2.7451 \times 10^{-23} \leq \frac{\lambda_{12}}{M_p} \leq 4.8039 \times 10^{-5}. \tag{22}$$

In addition, we estimate the value of $T_{\max}/T_{rh}$

$$\frac{T_{\max}}{T_{rh}} = \left(\frac{3}{8}\right)^{2/5} \left(\frac{3M_p}{\pi}\sqrt{\frac{10}{g_*}}\frac{\mathcal{H}_I}{T_{rh}^2}\right)^{1/4}, \tag{23}$$

and show the allowed ranges in Fig.6. Where the constraints of red dashed line is from the BBN $T_{rh} > 4MeV$ and the stability in the next section, $T_{rh} < 4.43 \times 10^{12}$GeV by the upper bound of λ_{12} in Eq.(29).

VI. RADIATIVE CORRECTIONS AND STABILITY

In order to ensure that the coupling terms added in the discussion of the reheating process in the previous section do not affect the inflationary dynamics at the CMB scale, and do not affect the generation of GWs at the second inflection point, thus do not affect the parameter space of the model, we analysis the stability of the inflation potential, calculate the one-loop CW correction of these coupling terms to the inflationary potential and restrict the coupling parameters.

The one-loop CW correction is [37, 38]

$$\Delta V = \sum_j \frac{g_j}{64\pi^2}(-1)^{2s_j}\tilde{m}_j^4\left[\ln\left(\frac{\widetilde{m}_j^2}{\mu^2}\right)-\frac{3}{2}\right], \tag{24}$$

and the corresponding first and second derivative of V_{CW} are

$$\begin{aligned} V'_{\rm CW} &= \sum_j \frac{g_j}{32\pi^2}(-1)^{2s_j}\tilde{m}_j^2\left(\widetilde{m}_j^2\right)'\left[\ln\left(\frac{\widetilde{m}_j^2}{\mu^2}\right)-1\right], \\ V''_{\rm CW} &= \sum_j \frac{g_j}{32\pi^2}(-1)^{2s_j}\left\{\left[\left(\left(\widetilde{m}_j^2\right)'\right)^2+\widetilde{m}_j^2\left(\widetilde{m}_j^2\right)''\right]\ln\left(\frac{\widetilde{m}_j^2}{\mu^2}\right)-\widetilde{m}_j^2\left(\widetilde{m}_j^2\right)''\right\}, \end{aligned} \tag{25}$$

where the index j is summing over three fields, the inflaton, the Higgs H and the fermion χ, and the spin s_j are $s_H=0, s_\chi=1/2, s_\phi=0$,the number of degrees of freedom of the fields are $g_H=4, g_\chi=4, g_\phi=0$, respectively. The renormalization scale μ is taken as ϕ_0. $\tilde{m}_j$ are field-dependent masses, and in our model they are given by

$$\begin{aligned} \widetilde{m}_\phi^2(\phi) &= \frac{6V_0}{\Lambda^6}\Big(5\phi^4-8(\alpha_2+1)\phi^3(\phi_1+\phi_2)+3\phi^2\left(\phi_1^2+4\phi_1\phi_2+\phi_2^2\right) \\ &\quad -4(\alpha_1+1)\phi\phi_1\phi_2(\phi_1+\phi_2)+\phi_1^2\phi_2^2\Big), \\ \widetilde{m}_\chi^2(\phi) &= \left(m_\chi+y_\chi\phi\right)^2, \\ \widetilde{m}_H^2(\phi) &= m_H^2+\lambda_{12}\phi. \end{aligned} \tag{26}$$

At the high scale inflection point ϕ_2, the first and second derivatives of inflation potential are

$$\begin{aligned} V'(\phi_2) &= -\frac{12V_0}{\Lambda^6}{\phi_2}^3(\phi_1+\phi_2)(\alpha_1\phi_1+\alpha_2\phi_2), \\ V''(\phi_2) &= -\frac{24V_0}{\Lambda^6}{\phi_2}^2(\phi_1+\phi_2)(\alpha_1\phi_1+2\alpha_2\phi_2), \end{aligned} \tag{27}$$

and at such point, the derivatives of the one-loop CW correction are

$$
\begin{aligned}
V'_{CW}(\phi_2) &= \frac{\lambda_{12}^2\phi_2(\ln\left(\frac{\lambda_{12}}{\phi_2}\right)-1)-2{\phi_2}^3y_\chi^4(\ln\left(y_\chi^2\right)-1)}{8\pi^2} \\
&+\frac{1}{\pi^2\Lambda^{12}}9{V_0}^2{\phi_2}^3\Big(\ln\left(-\frac{24V_0(\phi_1+\phi_2)(\alpha_1\phi_1+2\alpha_2\phi_3)}{\Lambda^6}\right)-1\Big)(\phi_1+\phi_2)(\alpha_1\phi_1+2\alpha_2\phi_2) \\
&\times((2\alpha_1-1){\phi_1}^2+2(1+\alpha_1+6\alpha_2)\phi_1\phi_2+(12\alpha_2-1){\phi_2}^2), \\
V''_{CW}(\phi_2) &= \frac{\lambda_{12}^2\ln\left(\frac{\lambda_{12}}{\phi_2}\right)+2{\phi_2}^2y_\chi^4(1-3\ln\left(y_\chi^2\right))}{8\pi^2} \\
&+\frac{1}{4\pi^2\Lambda^{12}}9{V_0}^2{\phi_2}^2\Big(3((1-2\alpha_1){\phi_1}^2-2(1+\alpha_1+6\alpha_2)\phi_1\phi_2+(1-12\alpha_2){\phi_2}^2)^2 \\
&-6(\phi_1+\phi_2)(\alpha_1\phi_1+2\alpha_2\phi_2)({\phi_1}^2+(3-8\alpha_2){\phi_2}^2-4\phi_1(\phi_2+2\alpha_2\phi_2)) \\
&+2((1-2\alpha_1){\phi_1}^2-2(1+\alpha_1+6\alpha_2)\phi_1\phi_2+(1-12\alpha_2){\phi_2}^2)^2 \\
&\times(\ln\left(-\frac{24V_0(\phi_1+\phi_2)(\alpha_1\phi_1+2\alpha_2\phi_2)}{\Lambda^6}\right)-\frac{3}{2}) \\
&-6(\phi_1+\phi_2)(\alpha_1\phi_1+2\alpha_2\phi_2)({\phi_1}^2+(3-8\alpha_2){\phi_2}^2-4\phi_1(\phi_2+2\alpha_2\phi_2)) \\
&\times(2\ln\left(-\frac{24V_0(\phi_1+\phi_2)(\alpha_1\phi_1+2\alpha_2\phi_2)}{\Lambda^6}\right)-3)\Big).
\end{aligned}
\tag{28}
$$

In order to make sure the addition coupling terms do not effect the inflation dynamics, we need to make sure that the terms of y_χ^4 and λ_{12}^2 are much smaller than the tree-level results(27), which will give the following restrictions on the parameters spaces

$$
\begin{aligned}
y_\chi &< 1.00687\times10^{-4}, \\
\lambda_{12} &< 3.03996\times10^{-8}M_p, \\
y_\chi &< 1.8046\times10^{-4}, \\
\lambda_{12} &< 1.73968\times10^{-7}M_p.
\end{aligned}
\tag{29}
$$

In addition, in our model we must also need to ensure that the addition coupled terms will not affect the generation of GWs, that is, the corresponding terms of y_χ^4 and λ_{12}^2 in the

one-loop CW corrections at the low scale inflection point

$$
\begin{aligned}
V'_{CW}(\phi_2) &= \frac{{\lambda_{12}}^2\phi_1(\ln\left(\frac{\lambda_{12}}{\phi_1}\right)-1)-2{\phi_1}^3(\ln\left(y_\chi^2\right)-1)y_\chi^4}{8\pi^2} \\
&+\frac{1}{\pi^2\Lambda^{12}}9{V_0}^2{\phi_1}^3(\ln\left(-\frac{24V_0(\phi_1+\phi_2)(2\alpha_2\phi_1+\alpha_1\phi_2)}{\Lambda^6}\right)-1)(\phi_1+\phi_2)(2\alpha_2\phi_1+\alpha_1\phi_2) \\
&\times((12\alpha_2-1){\phi_1}^2+2(1+\alpha_1+6\alpha_2)\phi_1\phi_2+(2\alpha_1-1){\phi_2}^2), \\
V''_{CW}(\phi_2) &= \frac{({\lambda_{12}}^2\ln\left(\frac{\lambda_{12}}{\phi_1}\right)-2{\phi_1}^2(3\ln\left(y_\chi^2\right)-1)y_\chi^4)}{8\pi^2} \\
&+\frac{1}{4\pi^2\Lambda^{12}}9{V_0}^2{\phi_1}^2\Big(3((1-12\alpha_2){\phi_1}^2-2(1+\alpha_1+6\alpha_2)\phi_1\phi_2+(1-2\alpha_1){\phi_2}^2)^2 \\
&+6(\phi_1+\phi_2)(2\alpha_2\phi_1+\alpha_1\phi_2)((-3+8\alpha_2){\phi_1}^2-{\phi_2}^2+4\phi_1(\phi_2+2\alpha_2\phi_2)) \\
&+2((1-12\alpha_2){\phi_1}^2-2(1+\alpha_1+6\alpha_2)\phi_1\phi_2+(1-2\alpha_1){\phi_2}^2)^2 \\
&\times(\ln\left(-\frac{24V_0(\phi_1+\phi_2)(2\alpha_2\phi_1+\alpha_1\phi_2)}{\Lambda^6}\right)-\frac{3}{2}) \\
&+6(\phi_1+\phi_2)(2\alpha_2\phi_1+\alpha_1\phi_2)((-3+8\alpha_2){\phi_1}^2-{\phi_2}^2+4\phi_1(\phi_2+2\alpha_2\phi_2)) \\
&\times(2\ln\left(-\frac{24V_0(\phi_1+\phi_2)(2\alpha_2\phi_1+\alpha_1\phi_2)}{\Lambda^6}\right)-3)\Big),
\end{aligned}
\tag{30}
$$

are much smaller than the terms of tree-level

$$
\begin{aligned}
V'(\phi_1) &= -\frac{12V_0}{\Lambda^6}{\phi_1}^3(\phi_1+\phi_2)(\alpha_2\phi_1+\alpha_1\phi_2), \\
V''(\phi_1) &= -\frac{24V_0}{\Lambda^6}{\phi_1}^2(\phi_1+\phi_2)(2\alpha_2\phi_1+\alpha_1\phi_2),
\end{aligned}
\tag{31}
$$

which will give the following restrictions

$$
\begin{aligned}
y_\chi &< 2.2307\times10^{-4}, \\
\lambda_{12} &< 6.46594\times10^{-8}M_p, \\
y_\chi &< 1.88144\times10^{-4}, \\
\lambda_{12} &< 8.18895\times10^{-8}M_p.
\end{aligned}
\tag{32}
$$

Combine 29 and 32, we get the upper bounds are $y_\chi < 1.00687\times10^{-4}$ and $\lambda_{12} < 3.03996\times10^{-8}M_p$. Plugging the upper limit of λ_{12} into (20), we can give an upper limit on the reheating temperature $T_{rh} < 4.43\times10^{12}$GeV.

VII. DARK MATTER PRODUCTION AND RELIC DENSITY

In this section, we will study the dark matter production during reheating. Combining the Boltzmann equation of DM number density n_χ and the Friedman equation, and considering that during $T_{rh} < T < T_{max}$ the energy density is dominated by the inflaton, then we can obtain the following relationship between the comoving number density $N = n_\chi a^3$ of DM and the reheating temperature T_{rh} as[73]

$$\frac{dN}{dT} = -\frac{8}{\pi}\sqrt{\frac{10}{g_*}}\frac{M_p T_{\rm rh}^{10}}{T^{13}} a^3\left(T_{\rm rh}\right)\gamma, \tag{33}$$

where a is the scale factor and γ is the density of DM production rate. And then the DM yield $Y \equiv n_\chi/s$ can be expressed as

$$\frac{dY}{dT} = -\frac{135}{2\pi^3 g_{*,s}}\sqrt{\frac{10}{g_*}}\frac{M_p}{T^6}\gamma, \tag{34}$$

where $s \equiv \frac{2\pi^2}{45} g_{*,s} T^3$is the entropy density at temperature T, and $g_{*,s}$ is the number of relativistic degrees of freedom contributing to the SM entropy [78]. In addition, it is worth to note that in order to consistent with observations of DM energy density , the present day DM yield is fixed by[73]

$$m_\chi Y_0 \simeq 4.3 \times 10^{-10}\text{GeV}. \tag{35}$$

After inflation, the DM can produced by the direct decay of inflatons, the 2-to-2 scattering of inflatons and the 2-to-2 scattering of SM particles.

The main way of dark matter production is the direct decay of inflatons, in this case, the DM production rate density is

$$\gamma = 2\text{Br}\Gamma\frac{\rho}{m}. \tag{36}$$

Using Eq. (34), we can get that the corresponding DM yield in this case is

$$Y_0 \simeq \frac{3}{\pi}\frac{g_*}{g_{*,s}}\sqrt{\frac{10}{g_*}}\frac{M_p\Gamma}{m_\phi T_{\rm rh}}\text{Br} \simeq 1.163 \times 10^{-2} M_p \frac{y_\chi^2}{T_{rh}}, \tag{37}$$

In the above equation we have assume that $g_{*,s} = g_*$. Combined with Eq.(35), we obtain the conditions if the inflatons decay constitutes the whole DM abundance, and show the allowed range of the coupling coefficient y_χ in Fig. 7. Where the constraints of purple region

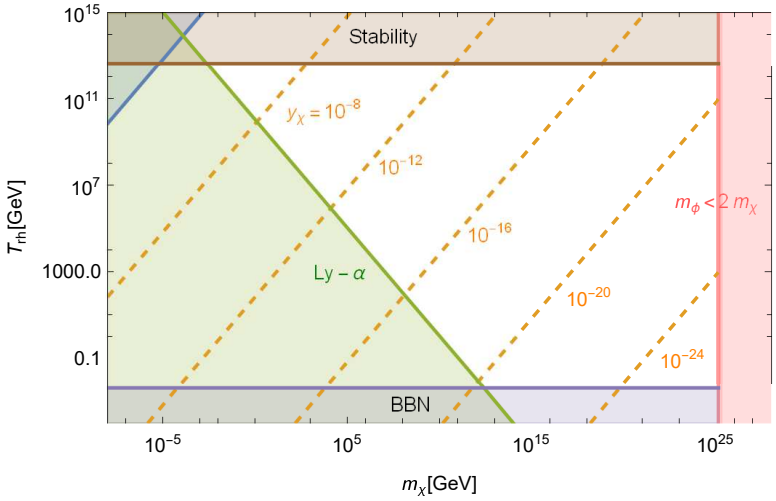


FIG. 7: The allowed range of coupling parameters y_χ when the direct decay of the inflaton produces the whole DM.

is from the BBN, $T_{rh} > 4MeV$, the brown and blue region are from the upper bound of $T_{rh} < 4.43 \times 10^{12}$Gev by the discussion of stability in Section 6, the green region is from the $Lyman - \alpha$ bound $\frac{m_\chi}{keV} \geq \frac{2m_\phi}{T_{rh}}$ [73], the red region is from the kinematical threshold $m_\phi > 2m_\chi$. From Fig. 7 we can further get that if inflatons decay process constitutes all the DM, the parameter y_χ should satisfies $2.081 \times 10^{-27} < y_\chi < 5.294 \times 10^{-6}$.

Secondly, dark matter can be produced by the 2-to-2 scatter of the inflaton. In this case [79–81]

$$\gamma = \frac{\pi^3 g_*^2}{3686400} \frac{T^{16}}{M_p^4 T_{\rm rh}^8} \frac{m_\chi^2}{m_\phi^2} \left(1 - \frac{m_\chi^2}{m_\phi^2}\right)^{3/2}, \tag{38}$$

and the the corresponding DM yield is

$$\begin{aligned} Y_0 &\simeq \frac{g_*^2}{81920 g_{*,s}} \sqrt{\frac{10}{g_*}} \left(\frac{T_{\rm rh}}{M_p}\right)^3 \left[\left(\frac{T_{\rm max}}{T_{\rm rh}}\right)^4 - 1\right] \frac{m_\chi^2}{m_\phi^2} \left(1 - \frac{m_\chi^2}{m_\phi^2}\right)^{3/2} \\ &\simeq 1.8 \times 10^{-2} \frac{T_{\rm rh} m_\chi^2}{M_p^{5/2} m_\phi^{1/2}} \left(1 - \frac{m_\chi^2}{m_\phi^2}\right)^{3/2}. \end{aligned} \tag{39}$$

Combine with the upper bound of $T_{rh} < 4.43 \times 10^{12}$GeV in section 6, we get that for reasonable values of m_χ, the DM yield Y_0 is less than 10^{-18}, the contribution to DM abundance is negligible.

Thirdly, dark matter can also be produced via the 2-to-2 scattering of SM particles, mediated by gravitons or inflatons. For gravitons act as mediators, one can get the decay rate density is [82–84]

$$\gamma(T) = \alpha \frac{T^8}{M_p^4}, \tag{40}$$

with $\alpha \simeq 1.1 \times 10^{-3}$. The corresponding DM Yield through this channel is

$$Y_0 = \begin{cases} \frac{45\alpha}{2\pi^3 g_{*,s}} \sqrt{\frac{10}{g_*}} \left(\frac{T_{rh}}{M_p}\right)^3, & \text{for } m_\chi \ll T_{rh}, \\ \frac{45\alpha}{2\pi^3 g_{*,s}} \sqrt{\frac{10}{g_*}} \frac{T_{rh}^7}{M_p^3 m_\chi^4}, & \text{for } T_{rh} \ll m_\chi \ll T_{\max}. \end{cases} \tag{41}$$

Similarly, if the mediators are inflatons, we can get

$$\gamma(T) \simeq \frac{y_\chi^2 \lambda_{12}^2}{2\pi^5} \frac{T^6}{m_\phi^4}, \tag{42}$$

and the dark matter Yield is

$$Y_0 \simeq \frac{135 y_\chi^2 \lambda_{12}^2}{4\pi^8 g_{*,s}} \sqrt{\frac{10}{g_*}} \frac{M_p T_{rh}}{m_\phi^4}, \quad \text{for } T_{rh} \ll m_\phi. \tag{43}$$

Using the upper bound of y_χ, λ_{12} and T_{rh} in section 6, we carry out numerical calculation on Y_0, and for the graviton mediation the maximum value is on the order of $Y_0 \sim 10^{-23}$ for $m_\chi \ll T_{rh}$, $Y_0 \sim 10^{-25}$ for $T_{rh} \ll m_\chi \ll T_{\max}$, and for the inflatons as the mediators, the maximum value is $Y_0 \sim 10^{-48}$, which are all very small compared to the present DM density, so that we can ignore both cases of the 2-to-2 scattering processes.

Moreover, when the scalar perturbations corresponding to the peak of the power spectrum renter the horizon, it will produce the primordial black hole(PBHs) through gravitational collapse, which could also be a candidate of DM [85–90]. Thus we also calculate the abundance of PBHs using the Press-Schechter approach of gravitational collapse, and found that the peak mass of PBHs is around $0.7 M_\odot$ and the fraction in dark matter is about 10^{-33}, which is very small and can be negligible.

VIII. SUMMARY

In this paper we discuss the explanation of NANOGrav data using inflationary potential with double-inflection-point, and such potential can be realized by the polynomial potential

from effective field theory with a cut off scale. For some choices of parameter sets, we analyze the inflation dynamics and show that the inflection point at the high scale predicts a scale-invariant power spectrum which consistent with the observations of the CMB. On the other hand, the inflection point at the low scale can cause an ultra-slow-roll stage, which will generate a peak in the scalar power spectrum, the height of which is about 10^7 magnitude of the CMB scale power spectrum. When the perturbations corresponding to the peak value re-enters the horizon, it will induce GWs that can be detected by experiments. We calculate the energy spectrum of GWs and shown that the peak is at frequencies around nanohertz, which is within the frequency range of SKA and EPTA, and lies in the 2σ uncertainty of the NANOGrav constraints. In addition, around millihertz, the curves lies above the expected sensitivity curves of ASTROD-GW, so it can be detected in near future.

After inflation ends, we assume that the inflaton is coupled with SM Higgs boson and singlet fermionic dark matter field. We analyze the reheating temperature, calculate the effect of one-loop CW corrections of the coupling terms, combined with the bounds of BBN, Lyman-α, etc, we constraints the coupling parameters as $y_\chi < 1.00687 \times 10^{-4}$ and $2.7451 \times 10^{-23} < \lambda_{12}/M_p < 3.03996 \times 10^{-8}$. We also discuss the dark matter production of inflaton decay, inflaton scattering and SM scattering, and find that the main way to produce dark matter is the direct decay of inflaton. If we assume that the inflaton decay process produce the whole DM abundance, the parameter y_χ should satisfies $2.081 \times 10^{-27} < y_\chi < 5.294 \times 10^{-6}$.

ACKNOWLEDGMENTS

This work was supported by "the National Natural Science Foundation of China" (NNSFC) with Grant No. 11705133, and by "the Natural Science Basis Research Plan in Shaanxi Province of China" No. 2023-JC-YB-072.

[1] Z. Arzoumanian *et al.* [NANOGrav], Astrophys. J. Lett. **905** (2020) no.2, L34 [arXiv:2009.04496 [astro-ph.HE]].

[2] V. Vaskonen and H. Veermäe, Phys. Rev. Lett. **126** (2021) no.5, 051303 [arXiv:2009.07832 [astro-ph.CO]].

[3] K. Kohri and T. Terada, Phys. Lett. B **813** (2021), 136040 [arXiv:2009.11853 [astro-ph.CO]].

[4] V. De Luca, G. Franciolini and A. Riotto, Phys. Rev. Lett. **126** (2021) no.4, 041303 [arXiv:2009.08268 [astro-ph.CO]].

[5] M. Kawasaki and H. Nakatsuka, [arXiv:2101.11244 [astro-ph.CO]].

[6] S. Vagnozzi, Mon. Not. Roy. Astron. Soc. **502** (2021) no.1, L11-L15 [arXiv:2009.13432 [astro-ph.CO]].

[7] G. Domènech and S. Pi, [arXiv:2010.03976 [astro-ph.CO]].

[8] S. Matarrese, S. Mollerach and M. Bruni, Phys. Rev. D **58**, 043504 (1998) [astro-ph/9707278].

[9] V. Acquaviva, N. Bartolo, S. Matarrese and A. Riotto, Nucl. Phys. B **667**, 119 (2003) [astro-ph/0209156].

[10] H. Assadullahi and D. Wands, Phys. Rev. D **79**, 083511 (2009) [arXiv:0901.0989 [astro-ph.CO]].

[11] L. Alabidi, K. Kohri, M. Sasaki and Y. Sendouda, JCAP **1209**, 017 (2012) [arXiv:1203.4663 [astro-ph.CO]].

[12] L. Alabidi, K. Kohri, M. Sasaki and Y. Sendouda, JCAP **1305**, 033 (2013) [arXiv:1303.4519 [astro-ph.CO]].

[13] K. Kohri and T. Terada, Phys. Rev. D **97**, no. 12, 123532 (2018) [arXiv:1804.08577 [gr-qc]].

[14] R. G. Cai, S. Pi and M. Sasaki, Phys. Rev. Lett. **122**, no. 20, 201101 (2019) [arXiv:1810.11000 [astro-ph.CO]].

[15] K. Inomata and T. Nakama, Phys. Rev. D **99**, no. 4, 043511 (2019) [arXiv:1812.00674 [astro-ph.CO]].

[16] R. G. Cai, S. Pi, S. J. Wang and X. Y. Yang, arXiv:1901.10152 [astro-ph.CO].

[17] J. Fumagalli, S. Renaux-Petel and L. T. Witkowski, [arXiv:2012.02761 [astro-ph.CO]].

[18] J. Garcia-Bellido, M. Peloso and C. Unal, JCAP **09** (2017), 013 [arXiv:1707.02441 [astro-ph.CO]].

[19] C. Unal, Phys. Rev. D **99** (2019) no.4, 041301 [arXiv:1811.09151 [astro-ph.CO]].

[20] G. Domènech, Int. J. Mod. Phys. D **29** (2020) no.03, 2050028 [arXiv:1912.05583 [gr-qc]].

[21] G. Domènech and M. Sasaki, Phys. Rev. D **103** (2021) no.6, 063531 [arXiv:2012.14016 [gr-qc]].

[22] G. Domènech, [arXiv:2109.01398 [gr-qc]].

[23] J. Garcia-Bellido and E. Ruiz Morales, Phys. Dark Univ. **18**, 47 (2017) [arXiv:1702.03901 [astro-ph.CO]].

[24] C. Germani and T. Prokopec, Phys. Dark Univ. **18**, 6-10 (2017) [arXiv:1706.04226 [astro-ph.CO]].

[25] H. Di and Y. Gong, JCAP **1807**, no. 07, 007 (2018) [arXiv:1707.09578 [astro-ph.CO]].

[26] Guillermo Ballesteros, Marco Taoso. Phys.Rev. D97 (2018) no.2, 023501. [arXiv:1709.05565]

[27] I. Dalianis, A. Kehagias and G. Tringas, JCAP **1901**, 037 (2019) [arXiv:1805.09483 [astro-ph.CO]].

[28] T. J. Gao and X. Y. Yang, Int. J. Mod. Phys. A **34** (2019) no.32, 1950213

[29] J. M. Ezquiaga, J. Garcia-Bellido and E. Ruiz Morales, Phys. Lett. B **776**, 345-349 (2018) [arXiv:1705.04861 [astro-ph.CO]].

[30] F. Bezrukov, M. Pauly and J. Rubio, JCAP **02**, 040 (2018) [arXiv:1706.05007 [hep-ph]].

[31] M. Drees and Y. Xu, arXiv:1905.13581 [hep-ph].

[32] O. Özsoy, S. Parameswaran, G. Tasinato and I. Zavala, JCAP **07**, 005 (2018) [arXiv:1803.07626 [hep-th]].

[33] T. J. Gao and X. Y. Yang, Int. J. Mod. Phys. A **34**, no.32, 1950213 (2019)

[34] M. Cicoli, V. A. Diaz and F. G. Pedro, JCAP **06**, 034 (2018) doi:10.1088/1475-7516/2018/06/034 [arXiv:1803.02837 [hep-th]].

[35] J. Liu, Z. K. Guo and R. G. Cai, Phys. Rev. D **101**, no.8, 083535 (2020) [arXiv:2003.02075 [astro-ph.CO]].

[36] Y. Akrami *et al.* [Planck Collaboration], arXiv:1807.06211 [astro-ph.CO].

[37] S.R. Coleman and E.J. Weinberg, Radiative Corrections as the Origin of Spontaneous Symmetry Breaking, Phys. Rev. D 7 (1973) 1888.

[38] E. J. Weinberg, [arXiv:hep-th/0507214 [hep-th]].

[39] S. Sarkar, Big bang nucleosynthesis and physics beyond the standard model, Rept. Prog. Phys. 59 (1996) 1493 [hep-ph/9602260].

[40] M. Kawasaki, K. Kohri and N. Sugiyama, MeV scale reheating temperature and thermalization

of neutrino background, Phys. Rev. D 62 (2000) 023506 [astro-ph/0002127].

[41] S. Hannestad, What is the lowest possible reheating temperature?, Phys. Rev. D 70 (2004) 043506 [astro-ph/0403291].

[42] F. De Bernardis, L. Pagano and A. Melchiorri, New constraints on the reheating temperature of the universe after WMAP-5, Astropart. Phys. 30 (2008) 192.

[43] P.F. de Salas, M. Lattanzi, G. Mangano, G. Miele, S. Pastor and O. Pisanti, Bounds on very low reheating scenarios after Planck, Phys. Rev. D 92 (2015) 123534 [1511.00672].

[44] I. Masina, Dark matter and dark radiation from evaporating primordial black holes, Eur. Phys. J. Plus 135 (2020) 552 [2004.04740].

[45] V. Iršič et al., New Constraints on the free-streaming of warm dark matter from intermediate and small scale Lyman- forest data, Phys. Rev. D 96 (2017) 023522 [1702.01764].

[46] N. Bhaumik and R. K. Jain, JCAP **01**, 037 (2020) [arXiv:1907.04125 [astro-ph.CO]].

[47] K. Enqvist and A. Mazumdar, Phys. Rept. **380**, 99-234 (2003) [arXiv:hep-ph/0209244 [hep-ph]].

[48] C. P. Burgess, H. M. Lee and M. Trott, JHEP **09**, 103 (2009) [arXiv:0902.4465 [hep-ph]].

[49] F. Marchesano, G. Shiu and A. M. Uranga, JHEP **09**, 184 (2014) [arXiv:1404.3040 [hep-th]].

[50] M. P. Hertzberg, M. Yamada Phys. Rev. D 97, 083509 (2018) [arXiv:1712.09750 [astro-ph.CO]]

[51] G. Ballesteros, J. Rey, M. Taoso and A. Urbano JCAP 07 (2020) 025 [arXiv:2001.08220 [astro-ph.CO]]

[52] C. Germani and T. Prokopec, Phys. Dark Univ. **18**, 6 (2017) [arXiv:1706.04226 [astro-ph.CO]].

[53] K. Dimopoulos, Phys. Lett. B **775**, 262 (2017) [arXiv:1707.05644 [hep-ph]].

[54] J. M. Ezquiaga and J. Garca-Bellido, JCAP 1808 (2018) 018, [arXiv:1805.06731 [astro-ph]].

[55] D. Cruces, C. Germani and T. Prokopec, JCAP 1903 (2019) no.03, 048 , [arXiv:1807.09057 [gr-qc]].

[56] D. J. Schwarz, C. A. Terrero-Escalante and A. A. Garcia, Phys. Lett. B **517**, 243 (2001) [astro-ph/0106020].

[57] S. M. Leach, A. R. Liddle, J. Martin and D. J. Schwarz, Phys. Rev. D **66**, 023515 (2002) [astro-ph/0202094].

[58] D. J. Schwarz and C. A. Terrero-Escalante, JCAP **0408**, 003 (2004) [hep-ph/0403129].

[59] T. S. Bunch and P. C. W. Davies, Proc. Roy. Soc. Lond. A **360** (1978), 117-134

[60] C. T. Byrnes, P. S. Cole and S. P. Patil, JCAP **06**, 028 (2019) [arXiv:1811.11158 [astro-ph.CO]].

[61] D. Baumann, P. J. Steinhardt, K. Takahashi and K. Ichiki, Phys. Rev. D **76**, 084019 (2007) [hep-th/0703290].

[62] K. N. Ananda, C. Clarkson and D. Wands, Phys. Rev. D **75**, 123518 (2007) [gr-qc/0612013].

[63] K. Ando, K. Inomata, M. Kawasaki, K. Mukaida and T. T. Yanagida, Phys. Rev. D **97** (2018) no.12, 123512 [arXiv:1711.08956 [astro-ph.CO]].

[64] H. Kodama and M. Sasaki, Prog. Theor. Phys. Suppl. **78**, 1 (1984).

[65] V. F. Mukhanov, H. A. Feldman and R. H. Brandenberger, Phys. Rept. **215**, 203 (1992).

[66] J. R. Espinosa, D. Racco, and A. Riotto JCAP 09 (2018) 012 [arXiv:1804.07732 [hep-ph]].

[67] H. Audley et al. [arxiv:1702.00786 [astro-ph.IM]].

[68] Z. K. Guo, R. G. Cai and Y. Z. Zhang, arXiv:1807.09495 [gr-qc].

[69] C. J. Moore, R. H. Cole and C. P. L. Berry, Class. Quant. Grav. 32 (2015) no.1, 015014, [arXiv:1408.0740 [gr-qc]].

[70] J. Luo et al. [TianQin Collaboration], Class. Quant. Grav. 33 (2016) no.3, 035010, [arXiv:1512.02076 [astro-ph.IM]].

[71] K. Kuroda, W. T. Ni and W. P. Pan, Int. J. Mod. Phys. D 24 (2015) no.14, 1530031, [arXiv:1511.00231 [gr-qc]].

[72] M. Drees and Y. Xu, JCAP **09**, 012 (2021) [arXiv:2104.03977 [hep-ph]].

[73] N. Bernal and Y. Xu, Eur. Phys. J. C **81**, no.10, 877 (2021) [arXiv:2106.03950 [hep-ph]].

[74] A. Ghoshal, G. Lambiase, S. Pal, A. Paul and S. Porey, JHEP **09**, 231 (2022) doi:10.1007/JHEP09(2022)231 [arXiv:2206.10648 [hep-ph]].

[75] D. J. H. Chung, E. W. Kolb and A. Riotto, Production of massive particles during reheating, Phys. Rev. D 60, 063504 (1999) [arXiv:hep-ph/9809453 [hep-ph]].

[76] G. F. Giudice, E. W. Kolb and A. Riotto, Largest temperature of the radiation era and its cosmological implications, Phys. Rev. D 64 (2001), 023508 [arXiv:hep-ph/0005123 [hep-ph]].

[77] N. Bernal, F. Elahi, C. Maldonado and J. Unwin, Ultraviolet Freeze-in and Non-Standard

Cosmologies, JCAP 11 (2019), 026 [arXiv:1909.07992 [hep-ph]]

[78] M. Drees, F. Hajkarim and E.R. Schmitz, The Effects of QCD Equation of State on the Relic Density of WIMP Dark Matter, JCAP 06 (2015) 025 [1503.03513].

[79] Y. Mambrini and K.A. Olive, Gravitational Production of Dark Matter during Reheating, 2102.06214.

[80] N. Bernal and C.S. Fong, Dark Matter and Leptogenesis from Gravitational Production, 2103.06896.

[81] B. Barman and N. Bernal, Gravitational SIMPs, 2104.10699.

[82] M. Garny, M. Sandora and M.S. Sloth, Planckian Interacting Massive Particles as Dark Matter, Phys. Rev. Lett. 116 (2016) 101302 [1511.03278].

[83] Y. Tang and Y.-L. Wu, On Thermal Gravitational Contribution to Particle Production and Dark Matter, Phys. Lett. B 774 (2017) 676 [1708.05138].

[84] N. Bernal, M. Dutra, Y. Mambrini, K. Olive, M. Peloso and M. Pierre, Spin-2 Portal Dark Matter, Phys. Rev. D 97 (2018) 115020 [1803.01866].

[85] J. Yokoyama, Astron. Astrophys. **318**, 673 (1997) [astro-ph/9509027].

[86] J. Garcia-Bellido, A. D. Linde and D. Wands, Phys. Rev. D **54**, 6040 (1996) [astro-ph/9605094].

[87] S. Clesse and J. Garcia-Bellido, Phys. Rev. D **92**, no. 2, 023524 (2015) [arXiv:1501.07565 [astro-ph.CO]].

[88] J. Garcia-Bellido, M. Peloso and C. Unal, JCAP **1612**, no. 12, 031 (2016) [arXiv:1610.03763 [astro-ph.CO]].

[89] S. L. Cheng, W. Lee and K. W. Ng, JHEP **1702**, 008 (2017) [arXiv:1606.00206 [astro-ph.CO]].

[90] C. Fu, P. Wu and H. Yu, arXiv:1907.05042 [astro-ph.CO].